Proposal and Comparison of Trajectory Tracking Strategies for Mobile Robots

Valentim Ernandes Neto, Rafael H. M. Fonseca, and Alexandre Santos Brandão

***Abstract*— This work aims to propose and compare trajectory tracking controllers for mobile robots. At first the mathematical requirements to propose a feasible strategy for a unicycle-like robot are presented, as well as the necessary condition to guarantee the stability in the sense of Lyapunov. In the sequence, the controllers are tuned in simulation and then validated in real experiments. The performance indexes IAE, ITAE and IASC are used to compare four strategies, detailed in the text.**

I. Introduction

Robotics is intriguing, because includes several areas of knowledge, such as electronics, mechanics, linear and non-linear control theory and programming [1]. There are endless applications of mobile robotics in the contemporary world, ranging from the arts to military and industrial projects. Mobile robots are being used in dance presentations and performances with humans [2]. They are also used in the nuclear industry in situations that pose danger [3]. A similar use occurs in military operations, such as those of the United States in Afghanistan and Iraq.

In the literature, the usage of mobile robots has the posture and trajectory controls as fundamental problems. Numerous strategies are presented to solve these questions [4]. The trajectory control is defined as path following with time constraint [5]. New techniques are shown and implemented to optimize trajectory tracking controllers in mobile robots, even considering kinematic disturbance, uncertainties and/or discretization [6], [7], [8]. In addition, intelligent gain tuning to improve the velocity control can also be considered [9]. Therefore, it motivates the proposal of new optimized controllers, using nonlinear control laws.

This work aims to propose four different trajectory tracking strategies, and compare them. First, the gain tuning is performed by simulation, and then practical experiments are run to compare the controllers. Finally, statistical data indicates the performance of each controller.

This paper is split into the following sections: Section II describes the kinematic model, Section III analyzes the controllers' stability in the sense of Lyapunov. Section IV shows the performance indexes (IAE, ITAE and IASC) used to evaluate the experiment. Section V describes the controllers' tunning and Section VI describes the experiments run for data collection and validation. Section VII presents and discusses the results. Finally, Section VIII presents the final discussions, the contributions of this work, as well as proposals that should be addressed in future studies.

*This work was supported by CNPq and FAPEMIG.

Núcleo de Especialização em Robótica - NERO, Departamento de Engenharia Elétrica - DEL, Universidade Federal de Viçosa - UFV, Viçosa, MG - Brasil. E-mail: alexandre.brandao@ufv.br

978-1-5386-0956-9/17/$31.00 ©

II. The Kinematic Model of the Mobile Robot

Pioneer P3-DX mobile robot is a widespread research platform in the field of mobile robotics. It is a unicycle-like robot with differential drive. Fig. 1 illustrates its linear v and angular ω velocities, as well its current position $\mathbf{X} = [x\ y]^T$.

The angle ψ represents the robot orientation relative to the x-axis, and the parameter a is the distance between the point to be controlled and the midpoint of the virtual axis joining the wheels. The variable ρ is the distance between the robot and the desired position. The angle θ indicates the desired orientation when the robot reaches the goal. So the angle α is the robot angular error defined with the difference between θ and the current orientation ψ. The origin $\langle o \rangle$ of the inertial coordinate system is determined from the robot initial position.

Its kinematic model [7] is described by

$$\begin{bmatrix} \dot{x} \\ \dot{y} \\ \dot{\psi} \end{bmatrix} = \begin{bmatrix} \cos\psi & a\sin\psi \\ \sin\psi & a\cos\psi \\ 0 & 1 \end{bmatrix} \begin{bmatrix} v \\ \omega \end{bmatrix}. \tag{1}$$

Its compact form of the position kinematic model can be represented by

$$\dot{\mathbf{X}} = \mathbf{K}\mathbf{U}. \tag{2}$$

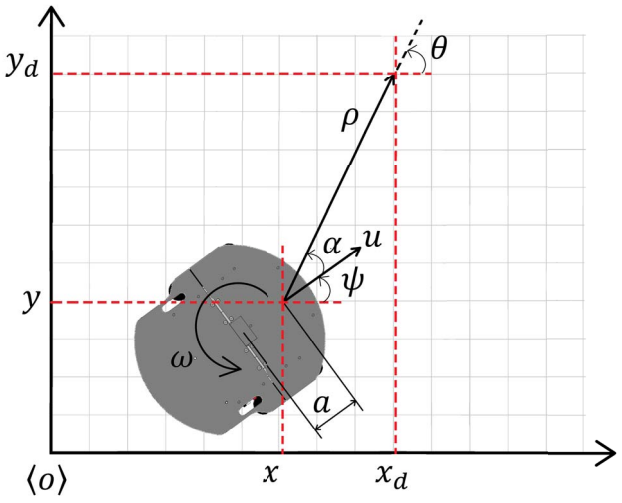

Fig. 1. Robot in search of the desired position.

III. Proposal and Stability Analysis of Trajectory Tracking Controllers

Based on the robot kinematic model, the position error can be defined as

$$\tilde{\mathbf{X}} = \mathbf{X}_d - \mathbf{X}. \tag{3}$$

Therefore, the error $\tilde{\mathbf{X}}$ consists in the difference between the desired position $\mathbf{X}_d$, and the current one $\mathbf{X}$. To guarantee the controller stability, we have a radially limited Lyapunov candidate function described by

$$V(\tilde{\mathbf{X}}) = \frac{1}{2}\tilde{\mathbf{X}}^T\tilde{\mathbf{X}} > 0. \tag{4}$$

Taking its first temporal derivative, we get

$$\dot{V}(\tilde{\mathbf{X}}) = \tilde{\mathbf{X}}^T\dot{\tilde{\mathbf{X}}}. \tag{5}$$

Replacing (2) and (3) into (5), we have

$$\dot{V}(\tilde{\mathbf{X}}) = \tilde{\mathbf{X}}^T(\dot{\mathbf{X}}_d - \mathbf{K}\mathbf{U}). \tag{6}$$

Adopting the control signal

$$\mathbf{U} = \mathbf{K}^{-1}(\dot{\mathbf{X}}_d + \mathbf{C}), \tag{7}$$

we finally get

$$\dot{V}(\tilde{\mathbf{X}}) = -\tilde{\mathbf{X}}^T\mathbf{C}. \tag{8}$$

Thus, the necessary condition to ensure controller stability is that $\mathbf{C}$ must be an odd function.

Therefore, the objective is to find a control strategy $\mathbf{C}$ such that $\dot{V}(\tilde{\mathbf{X}}) < 0, \forall\|\tilde{\mathbf{X}}\| > 0$. Note that, if the function describing the controller is odd, the stability criterion is satisfied. That way, four trajectory tracking controllers are proposed, defining their gain and saturation characteristics.

A. Hyperbolic Tangent

The first proposed controller basically consists of a proportional controller with a saturation function. The hyperbolic tangent function is an odd function, bounded upper and lower, which ensures an analytical control signal saturation. Moreover, it has an approximate linear behavior for small errors, in an area between saturation points. This strategy will be hereinafter called $\mathbf{u}_{\tanh}$, described by:

$$\mathbf{u}_{\tanh} = \mathbf{K}^{-1}\left[\dot{\mathbf{X}}_d + \mathbf{k}_1\tanh(\mathbf{k}_2\tilde{\mathbf{X}})\right] \tag{9}$$

The positive diagonal matrices $\mathbf{k}_1$ and $\mathbf{k}_2$, respectively, determine the degree of saturation of the control signals and the slope of the curve for small errors.

B. Inverse function of x

The second controller labeled $u_{1/x}$ is based on the fact that the inverse function has high values when the error is small, and vice-versa. Thus, this controller can further minimize small errors and, allied with the first controller, it has a wider range. Its proposal is mathematically described by

$$\mathbf{u}_{1/x} = \mathbf{K}^{-1}\left[\dot{\mathbf{X}}_d + \mathbf{k}_1\tanh(\mathbf{k}_2\tilde{\mathbf{X}}) + \mathbf{k}_3\tanh(\tilde{\mathbf{X}}\mathbf{k}_4\tilde{\mathbf{X}}^T)\tilde{\mathbf{X}}^{\#}\right] \tag{10}$$

where $\tilde{\mathbf{X}}^{\#} = \tilde{\mathbf{X}}(\tilde{\mathbf{X}}^T\tilde{\mathbf{X}})^T$. Notice that there is a saturated proportional controller represented by the first hyperbolic tangent, with saturation $\mathbf{k}_1$ and gain $\mathbf{k}_2$, added to another hyperbolic tangent in which the saturation is variable, depending on $\mathbf{k}_3$ and inversely proportional to the error value. In this second term the hyperbolic tangent argument has a gain $\mathbf{k}_4$ multiplied by the quadratic error. The gain matrices $\mathbf{k}_i$ are diagonal positives.

It is important to emphasize that the inverse function is odd. If it is multiplied by an even function $\tilde{\mathbf{X}}\mathbf{k}_4\tilde{\mathbf{X}}^T$, so the control signal can be considered an entirely odd function, and thus, its stability is guaranteed.

C. Exponential Function

The exponential function controller, $\mathbf{u}_{exp}$, also aims to provide a reasonable control signal for small error values. The function is indicated by:

$$\mathbf{u}_{exp} = \mathbf{K}^{-1}\left[\dot{\mathbf{X}}_d + \mathbf{k}_1(1 - e^{-k_2\|\tilde{\mathbf{X}}\|})\tilde{\mathbf{X}}\right] \tag{11}$$

Again, $\mathbf{k}_1$ is a positive definite diagonal matrix, and k_2 is a positive number. Notice that $\mathbf{k}_1$ adjusts the saturation value, while k_2 optimizes the time convergence.

D. Gaussian Function

The last proposed controller is based on the Gaussian function, very common on statistical analyzes. The first part of the controller uses the hyperbolic tangent, previously explained, to ensure a substantial, but limited, gain for large errors. The Gauss term maximizes the gain for small errors, which multiplied by the term k_3 and the error $\tilde{\mathbf{X}}$ acts as a variable gain proportional controller. This control signals are given by

$$\mathbf{u}_G = \mathbf{K}^{-1}\left[\dot{\mathbf{X}}_d + \mathbf{k}_1\tanh(\mathbf{k}_2\tilde{\mathbf{X}}) + \mathbf{k}_3 e^{-\tilde{\mathbf{X}}\mathbf{k}_4\tilde{\mathbf{X}}^T}\tilde{\mathbf{X}}\right] \tag{12}$$

Gaussian is an even function, and the function $\mathbf{k}_3\tilde{\mathbf{X}}$ is odd, so the control signal of this controller has the characteristics of an odd function. As higher the value of $\mathbf{k}_3$, the higher the controller's maximum overshot for small errors. In contrast, raising $\mathbf{k}_4$, the influence margin of large errors decreases.

IV. Performance Analysis

The controllers' performance is evaluated according to some indexes widely known in the literature. The IAE (Integral Absolute Error)

$$IAE = \int_0^{t_f} \|\tilde{\mathbf{X}}\|dt \tag{13}$$

provides the accumulation of error over time.

The ITAE (Integral Time-weighted Absolute Error)

$$ITAE = \int_0^{t_f} t\|\tilde{\mathbf{X}}\|dt \tag{14}$$

evaluates the value of the error in relation to the time, minimizing the initial errors and quantifying in greater scale the steady-state errors. In addition, as lower the ITAE values, as faster the system response.

The third index IASC (Integral Absolute Signal Control)

$$IASC = \int_0^{t_f} \|\mathbf{U}\|dt \tag{15}$$

allows to evaluate the amount of signal sent by the controller over time, informing the degree of actuation for the task to be performed.

V. Controller Adjustments

Initially, the gains of the $\mathbf{u}_{tanh}$ controller are tuned to obtain the lowest IAE, for sixty seconds of trajectory tracking in the curve described by

$$x = 3\sin\frac{3\pi}{80}t$$

$$y = \sin\frac{6\pi}{80}t$$

The other control strategies gains should be adjusted so that the value of the absolute integral of the error is very close to the $\mathbf{u}_{tanh}$'s IAE value. In this way, it would be possible to have a fixed parameter to evaluate the controllers performances analyzing other indexes (ITAE and IASC), as well as for other trajectory shapes.

To facilitate and expedite the gains adjustment, we use the MobileSim software to simulate the P3-DX robot before performing practical tests. After defining the gains, ten simulations are run for each controller, resulting in the statistical values expressed in Table I.

Then, to validate the gains through experiment, measurements are done in a flat environment without slopes, to guarantee the same ground conditions for each controller. Fig. 2 illustrates the parameterized trajectory, in which each controller is tested.

The average of the performance indexes and its respective standard deviations are shown in Table 2. Notice a proximity

TABLE I

Average values and standard deviation of performance indicators after gain tunning using MobileSim.

Controller	IAE	ITAE	IASC
Tanh	1.62 ± 0.04	26.7 ± 0.8	22.5 ± 0.08
InvX	1.61 ± 0.04	25.5 ± 0.8	23.0 ± 0.16
Exp	1.61 ± 0.03	27.0 ± 0.9	22.2 ± 0.07
Gauss	1.60 ± 0.02	26.6 ± 0.9	22.8 ± 0.09

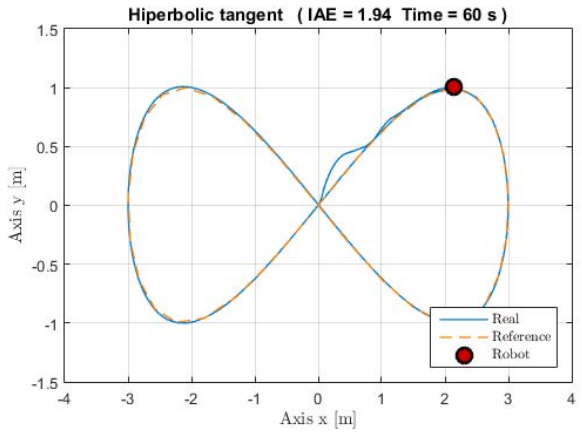

Fig. 2. Trajectory used to adjust controller gains.

of the values found in the simulation environment. In addition, the IAE average values of the controllers remained approximately the same. As result, the software used is highly recommended for gain adjustment and calculation of performance indicators, because the results are close to those one obtained in practice, when dealing with a flat environment without slopes.

From Table I and II, one can notice that $\mathbf{u}_G$ controller has the lowest ITAE value, followed by $\mathbf{u}_{1/x}$ and $\mathbf{u}_{exp}$. Apparently, $\mathbf{u}_G$ controller has a faster convergence, while $\mathbf{u}_{tanh}$ and $\mathbf{u}_{exp}$ have lesser controller performance over time, with the lower IASC values.

TABLE II

Average values and standard deviation of the performance indexes after experimental results.

Controller	IAE	ITAE	IASC
Tanh	1.94 ±0.05	27.3 ±0.3	22.1 ±0.05
InvX	1.87 ±0.06	26.7 ±0.3	22.5 ±0.13
Exp	1.88 ±0.05	26.8 ±0.4	22.1 ±0.04
Gauss	1.87 ±0.06	26.3 ±0.3	22.5 ±0.12

VI. Controller Comparison

To excite the controllers, on the real experiments, another trajectory shape is given:

$$\begin{cases} x = 3\sin\frac{3\pi}{80}t \\ y = \sin\frac{6\pi}{80}t \end{cases}, \quad 0s < t < 60s$$

$$\begin{cases} x = 5\cos\frac{4\pi}{80}(t-100) \\ y = 1.5\sin\frac{4\pi}{80}(t-100) \end{cases}, \quad 60s < t < 120s$$

The robot starts performing a lemniscate and then, it abruptly changes to an ellipse reference. Such a proposal allows a greater excitation of the controllers and a performance analysis for a longer time interval. In addition, the robot has moved at significant velocities and had to completely reverse its orientation during such reference change. Ten repetitions of the trajectory are performed for each one of the four controllers, to collect several measurements of IAE, ITAE and IASC.

VII. Results and Discussion

The path taken by the robot to each controller is shown in Fig. 3. The initial position of the robot is the origin of the Cartesian plane, and the red circle is the final robot position.

All the controllers have managed to stabilize. However, just checking the path traveled is not possible to conclude which controller is better in relation to the accumulated error or the response stabilization. It is necessary to estimate the mean and standard deviation of the performance indexes for a more conclusive result. These statistical measures are shown in Table III, and complemented by the normal distribution curves of the values collected in the experiment indicated in Fig 4.

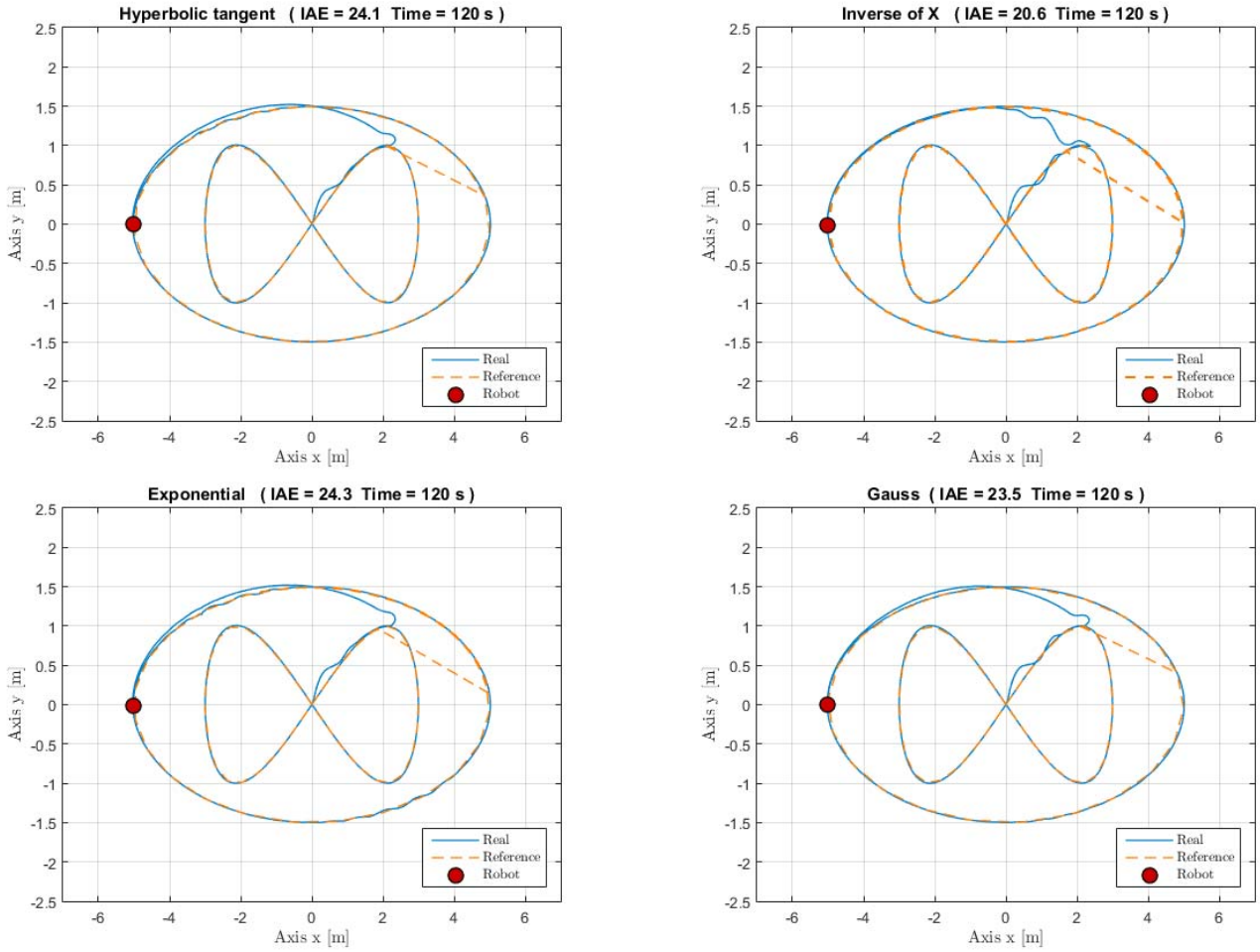

Fig. 3. Traveled trajectory for each controller.

TABLE III
AVERAGE VALUES AND STANDARD DEVIATION FOR EACH CONTROLLER.

Controller	IAE	ITAE	IASC
Tanh	24.06 ±0.09	1515 ±4	57.51 ±0.09
InvX	20.56 ±0.10	1275 ±5	59.68 ±0.52
Exp	24.33 ±0.08	1534 ±2	57.52 ±0.19
Gauss	23.50 ±0.05	1472 ±4	58.37 ±0.40

Visibly, $\mathbf{u}_{1/x}$ controller stays out in comparison with the others, having a smaller IAE (i.e., a smaller error accumulated over time), and a smaller ITAE (i.e., a faster convergence). The second-best controller, considering these parameters, is $\mathbf{u}_G$.

Considering the energy consumption, the two best controllers are also those that demanded more energy, since they have the highest IASC values. $\mathbf{u}_{tanh}$ and $\mathbf{u}_{exp}$ controllers have smaller and extremely close values.

It is important to note that even with a 3.7% higher IASC in relation to the lower value obtained for this index, the controller $\mathbf{u}_{1/x}$ provided an approximated reduction of 15% in IAE and 17% for ITAE, if compared to the other controllers.

Fig. 5 shows the graph of the error presented by the controllers as a function of time, as well as the variation of the linear and angular velocities performed by the robot during the experiment. It is noticeable from the variation of the error that all the controllers can converge to the desired trajectory and present an error close to zero. The controller $\mathbf{u}_{1/x}$ tends more quickly to the desired trajectory than the others. When evaluating the linear and angular velocities of the robot for the different controllers, it can be inferred that there is a greater overlap of the controller $\mathbf{u}_{1/x}$ in relation to the others, showing that it develops a greater speed to minimize the error in a shorter time.

All experiments can be seen in `youtu.be/8mRsEFxjALQ`. The video is in 4x velocity. One can notice all strategies behave in a similar way, however their differences can be check by the performance indexes.

VIII. Concluding Remarks

This paper proposes four different nonlinear trajectory tracking control strategies. Through simulations and experiments, using Pioneer 3D-DX robot, it is possible to adjust the gains of the controllers and prove their applicability. All controllers are able to follow the desired trajectory. Repetitive experiments are run, making possible to conclude that $\mathbf{u}_{1/x}$

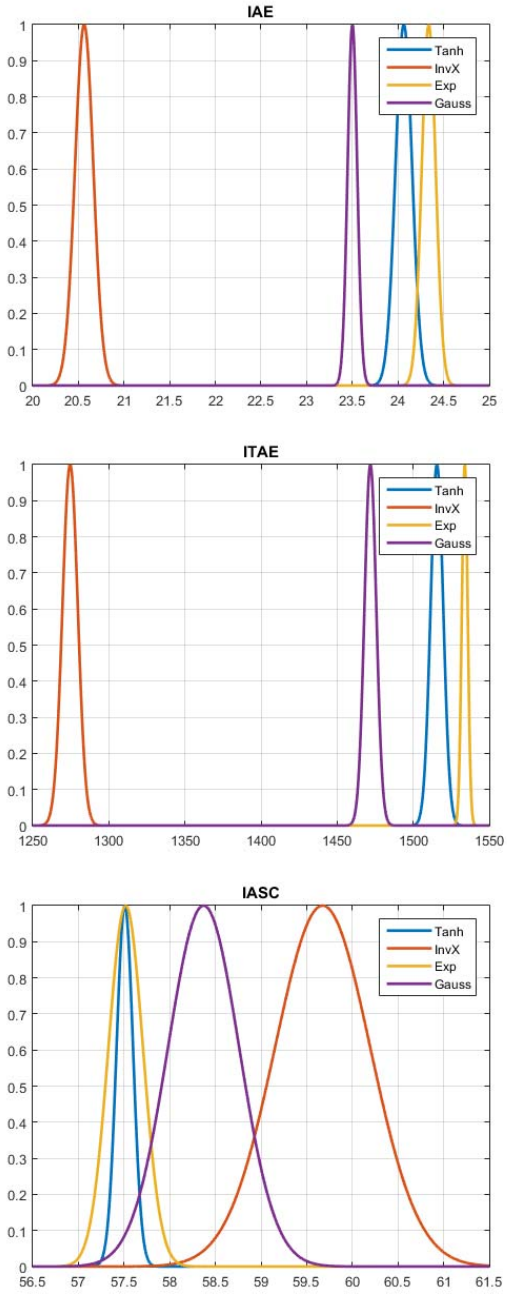

Fig. 4. Traveled trajectory for each controller.

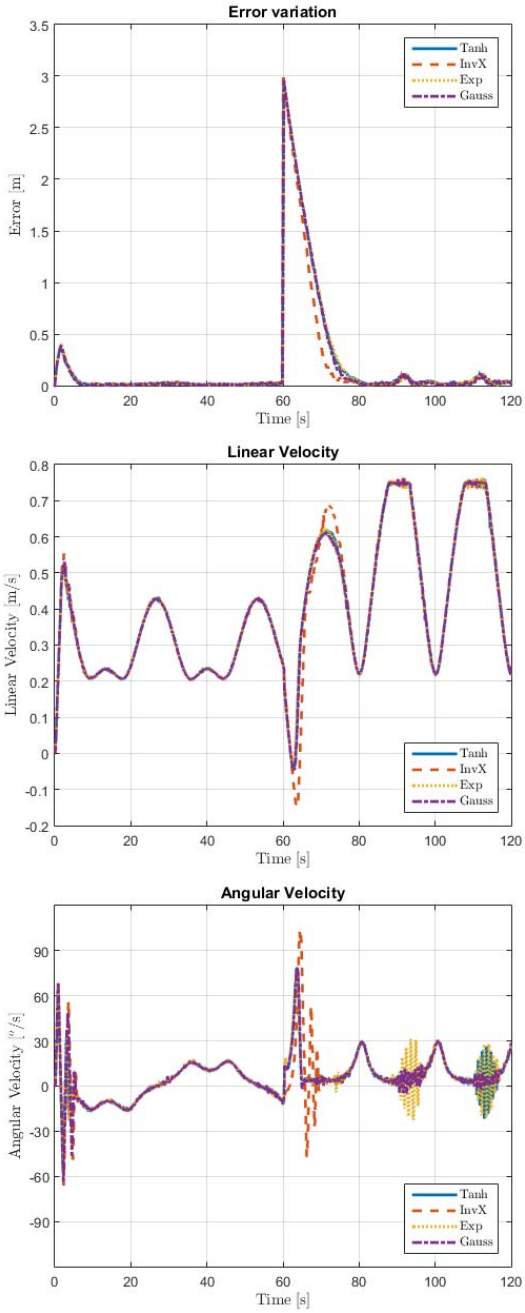

Fig. 5. Traveled trajectory for each controller.

controller is the most efficient in terms of error minimization and response speed, when compared among the others.

The data acquired by the simulations, using the software MobileSim, are close to the values found in the practice, in a flat environment and without slopes. Therefore, adjusted gains in the simulation are feasible and they can be used in real experiments.

For future works it is necessary to implement strategies to avoid obstacles to the trajectory controllers, so the mobile robot navigation will be closer to a real unstructured scenario. It is also suggested to verify the proposal applicability at higher speeds, with different dynamics.

IX. Acknowledgments

The authors thank CNPq and FAPEMIG for the awarded financial support. They also thank the Federal University of Viçosa for facilitating the realization of this project.

References

[1] H.-H. Huang, J.-H. Su, C.-S. Lee, J.-Y. Huang, and S.-H. Chuang, "Hands-on intelligent mobile robot laboratory with support from the industry," in *Education Engineering (EDUCON), 2010 IEEE*. IEEE, 2010, pp. 457–463.

[2] S. Tsuchida, T. Terada, and M. Tsukamoto, "A dance performance environment in which performers dance with multiple robotic balls," in *Proceedings of the 7th Augmented Human International Conference 2016*. ACM, 2016, p. 12.

[3] P. Dong, X. Wang, H. Xing, Y. Liu, and M. Zhang, "Design and control of a tracked robot for search and rescue in nuclear power plant," in *Advanced Robotics and Mechatronics (ICARM), International Conference on*. IEEE, 2016, pp. 330–335.

[4] A. Bessas, A. Benalia, and F. Boudjema, "Integral sliding mode control for trajectory tracking of wheeled mobile robot in presence of uncertainties," *Journal of Control Science and Engineering*, vol. 2016, 2016.

[5] Z. Li, J. Deng, R. Lu, Y. Xu, J. Bai, and C.-Y. Su, "Trajectory-tracking control of mobile robot systems incorporating neural-dynamic optimized model predictive approach," *IEEE Transactions on Systems, Man, and Cybernetics: Systems*, vol. 46, no. 6, pp. 740–749, 2016.

[6] E.-J. Hwang, H.-S. Kang, C.-H. Hyun, and M. Park, "Robust backstepping control based on a lyapunov redesign for skid-steered wheeled mobile robots," *International Journal of Advanced Robotic Systems*, vol. 10, no. 1, p. 26, 2013.

[7] L. Capito, P. Proaño, O. Camacho, A. Rosales, and G. Scaglia, "Experimental comparison of control strategies for trajectory tracking for mobile robots," *International Journal of Automation and Control*, vol. 10, no. 3, pp. 308–327, 2016.

[8] N. A. Martins, E. S. Elyoussef, D. W. Bertol, E. R. De Pieri, U. F. Moreno, and E. d. B. Castelan, "Trajectory tracking of a nonholonomic mobile robot with kinematic disturbances: a variable structure control design," *IEEE Latin America Transactions*, vol. 9, no. 3, pp. 276–283, 2011.

[9] C. Z. Resende, R. Carelli, and M. Sarcinelli-Filho, "A nonlinear trajectory tracking controller for mobile robots with velocity limitation via fuzzy gains," *Control Engineering Practice*, vol. 21, no. 10, pp. 1302–1309, 2013.